Geometrical and Stress Analysis of Factors Associated With Stent Fracture After Melody Percutaneous Pulmonary Valve Implantation

Daria Cosentino, PhD; Michael A. Quail, MBChB, MRCPCH, MSc; Giancarlo Pennati, PhD; Claudio Capelli, PhD; Philipp Bonhoeffer, MD; Vanessa Díaz-Zuccarini, PhD; Andrew M. Taylor, MD, FRCP, FRCR; Silvia Schievano, PhD

Percutaneous pulmonary valve implantation (PPVI) with the Melody device (Medtronic Inc, Minneapolis, MN) is an established, successful technique to treat pulmonary artery conduit dysfunction. Despite its success, a major technical issue related to the Melody device remains: stent fracture.[1] This problem has been reported to occur in as high as 25% of the treated patients[2,3] although <50% of the fractures require reintervention because of loss of stent structural integrity.[3–6] To minimize the risk of stent fracture, a prestenting strategy has been recommended, with the implantation of 1 or several bare metal stents (BMS) to create a scaffold for PPVI.[6–8] This has been shown to help reduce the risk of fracture.[7] However, despite the BMS, Melody stent fracture remains a problem and close clinical follow-up is required.[5]

Studies by Nordmeyer et al[2] and McElhinney et al[3] used 2-dimensional (2D) images from procedural and follow-up angiograms and x-rays to identify risk factors associated with stent fracture, which include PPVI in a native right ventricular outflow tract (RVOT) and in a noncalcified RVOT; the presence of PPVI recoil during balloon deflation; high ratio between the anteroposterior and the lateral PPVI diameter (largest/smallest), at the proximal level of the stent; severe RVOT obstruction; younger age; elevated pre- and postprocedural RVOT gradient; reduced conduit diameter; smaller ratio of the measured/original conduit diameter; and dynamic compression of the deployed valve and substantial apposition to the chest wall. These data indicate that mechanical factors related to the implant environment seem to play an important role in the stent fracture during and after device deployment.

The extreme morphological variability of PPVI implantation sites[9] often results in asymmetrical expansion of the

Received July 2, 2013; accepted June 23, 2014.

From the Department of Mechanical Engineering (D.C., V.D.-Z.), Institute of Cardiovascular Science and Great Ormond Street Hospital for Children (D.C., M.A.Q., C.C., A.M.T., S.S.), University College London, London, United Kingdom; Department of Chemical Engineering, Politecnico di Milano, Milan, Italy (G.P.); and Fondazione G. Monasterio, CNR–Regione Toscana, Pisa, Italy (P.B.).

Correspondence to Silvia Schievano, PhD, Cardiorespiratory Unit, Great Ormond Street Hospital for Children, Great Ormond St, London WC1N 3JH, United Kingdom. E-mail s.schievano@ucl.ac.uk

WHAT IS KNOWN

- Fracture of the stent frame of the Melody transcatheter pulmonary valve has been reported in as high as 25% of the treated patients.
- The causes of Melody valve stent fracture have not been fully identified, and the occurrence of this adverse event is likely because of a complex interaction among patient-related, implantation site-related, and device-related factors.

WHAT THE STUDY ADDS

- In this study, we categorized and evaluated 3D fundamental geometric and engineering parameters that could be derived for each patient from biplane fluoroscopy immediately after the procedure.
- Analysis of 3D reconstructions of the Melody stent from fluoroscopy images and computational simulations demonstrated that the probability of fracture decreased with preserved stent circularity after deployment and smaller compressive stresses generated during recoil.
- These findings help improve our understanding of stent fracture in this emerging clinical area.

Melody device,[10] and combined with the complex 3-dimensional (3D) deformations experienced by the stent during both deployment and cardiac cycle form the basis of stent mechanical failure. Therefore, a thorough analysis of these parameters may facilitate prediction of stent fracture with greater accuracy and precision. In this study, the in situ stent geometry and shape changes of Melody during implantation and the subsequent cardiac cycle were analyzed. In addition, a 3D patient-specific finite element (FE) analysis was performed, simulating device deployment and cyclic deformations during the cardiac cycle to identify parameters associated with stent fracture.

Methods

Patients Selection

Patients with PPVI treated in our center between 2007 and 2009 were retrospectively selected for this study (n=42; Table 1) if they fulfilled the following criteria: (1) PPVI procedure performed in a catheterization laboratory equipped with Axiom Artis Flat Panel Detector system (Siemens, Germany) to reduce image distortion;[10,11] (2) fluoroscopy images acquired with the arms of the fluoroscopy system positioned in the anteroposterior and lateral view, to have projections of the device in 2 orthogonal planes; (3) biplane fluoroscopic images available throughout the stent implantation phases from end of balloon inflation to ≥1 full cardiac cycle.

Two groups of patients were identified: the first (n=10) experienced fractures in the first year after successful PPVI; the second (n=32) had no adverse events in the same timeframe.

Stent fractures and their location were detected and assessed using routine x-ray images acquired after PPVI. In our center, patients with PPVI are routinely followed up at 1 and 6 months after the implantation, and if no problems are detected, at 1 year and on a yearly basis thereafter.

Table 1. Patients' Data (Average [Min, Max]) for the Fractured and Nonfractured Groups

	Fractured (n=10)	Nonfractured (n=32)
Age at implant, y	14 (10, 23)	19 (7, 71)
Sex (F/M)	4/6	11/21
BSA, m^2	1.48 (1.14, 1.90)	1.64 (0.90, 2.20)
Weight, kg	49.3 (32.9, 70.0)	58.2 (19.1, 106.0)
Primary indication stenosis or mixed disease[3]	6 (60%)	23 (72%)
Substantial apposition to chest wall[3]	2 (20%)	10 (31%)
Stent compression >1.1[3]	6 (60%)	19 (59%)
Dynamic compression[3]	1 (10%)	5 (16%)
Native right ventricular outflow tract[2]	0	0
No calcification[2]	4 (40%)	18 (56%)
Qualitative recoil[2]	5 (50%)	8 (25%)
Prestent*	4 (40%)	16 (50%)

*Three patients from the nonfractured group had 2 prestents. All the other patients had only 1 prestent.

The study had institutional approval and informed consent for the use of images and data for research purposes were given by the patients or their parent/guardian.

Reconstruction From Fluoroscopy Data

The orthogonal biplane fluoroscopy images of the device acquired during the procedure were postprocessed to reconstruct the in situ 3D stent geometry for every patient[10,12,13] (Figure 1A): the crown points (n=56) of the zigzag struts forming the stent were identified in both fluoroscopy images and then back-projected into the 3D space by tracing parallel rays (computer-aided design software Rhinoceros; McNeel and Associates, Seattle, WA). The intersection points between the rays determined the position of the strut junctions in 3D space. By joining these points with straight segments (n=96), the zigzag wires of the device were reproduced, and consequently the whole structure of the stent. Calibration of the fluoroscopy images was achieved by identifying the straightest strut of the stent in both projections and by scaling the images so that the reconstructed length (Figure 2A and 2B) of this strut (L_{rec}) was equal to the real length (L_{undef}=5.78 mm) of the undeformed stent struts. In 16 patients who underwent PPVI stent after dilatation, calibration was also further assessed using the markers of the Mullins balloon (NuMed Inc, Hopkinton, NY).

Using this methodology, the in situ stent configuration was reconstructed for each patient at 3 instants, including the end of the final balloon inflation (hereafter referred to as prerecoil), early systole and diastole (Figure 1B). The prerecoil was selected from the fluoroscopy images in the frame at the beginning of balloon deflation, whereas the systolic and the diastolic frames were identified according to the ECG tracing synchronized with the fluoroscopy acquisitions. For this patient population, the systolic and diastolic frames corresponded to the instants of maximum and minimum diameters during the cardiac cycle. The recoil process between the end of balloon inflation and the end of balloon deflation includes not only the intrinsic elastic recoil of the metal stent but also the recoil related to the arterial wall and surrounding tissues.

To quantify the reconstruction process error, the lengths of the reconstructed segments (L_{rec}) for each stent were plotted in a normal distribution. The metal stent struts cannot be visibly stretched during implantation; therefore, segments longer than the strut undeformed value (L_{undef}) represent errors of the reconstruction process. However, struts can be bent and, therefore, the reconstructed length can be smaller than L_{undef}. The portion of the graph below L_{undef} contains information about both bent struts and errors, and the average of the reconstructed segments is always smaller than L_{undef}. The reconstruction

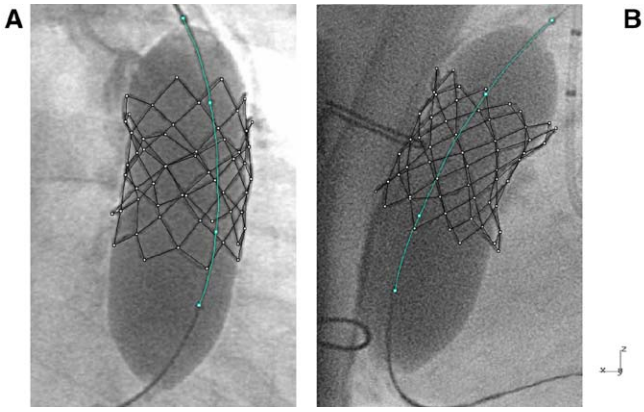

Figure 1. A, Stent 3-dimensional reconstruction using orthogonal biplane fluoroscopy images for 1 patient at the end of balloon expansion: anteroposterior and lateral projections. The markers of the post–percutaneous pulmonary valve implantation dilatation balloon are reconstructed in light blue. **B**, Three-dimensional stent geometry reconstructed from fluoroscopy images at the end of balloon expansion (black), systole (red), and diastole (blue) superimposed with the stent at its initial crimped configuration (green).

process error for each stent in each time step was calculated as $100\frac{L_{rec}-L_{undef}}{L_{undef}}$, measured for $L_{rec}>L_{undef}$.

Geometric Parameters

Three-dimensional stent shape and geometric variations after balloon deflation and during the cardiac cycle were compared between fractured and nonfractured patient groups. Four geometric parameters were defined to describe strut (96 per stent), cell (40 per stent), section (7 per stent), and stent configuration (Figure 2A).

- Strut length, L=distance between 2 junction points belonging to the same strut (Figure 2A and 2B).
- Circumferential asymmetry ratio, C_a=ratio between cell longitudinal, dl, and circumferential, dc, diagonals (Figure 2A).
- Radial asymmetry ratio, R_a=ratio between maximum section diameter D_{max} and minimum section diameter D_{min} (Figure 2B).
- Longitudinal asymmetry ratio, L_a=ratio between maximum and minimum standard diameter section D_{std}=diameter of the section if considered a circle with same section perimeter (Figure 2C).

All parameters were measured for each of the 3 reconstructed stent geometries per patient (prerecoil, systole, and diastole). Percentage variations of such parameters were calculated—named in the text as Δ parameter—during balloon deflation (recoil) as $100\times\frac{\text{prerecoil}-\text{systole}}{\text{prerecoil}}$ and during cardiac cycle as $100\times\frac{\text{systole}-\text{diastole}}{\text{systole}}$.

The following geometric parameters were inputted in the statistical fracture analysis per stent:

- at systole: L min, L aver, C_a min, C_a aver, R_a max, R_a aver, L_a
- during recoil and during cardiac cycle: ΔL max, ΔL aver, ΔC_a max, ΔC_a aver, ΔR_a max, ΔR_a aver, ΔL_a.

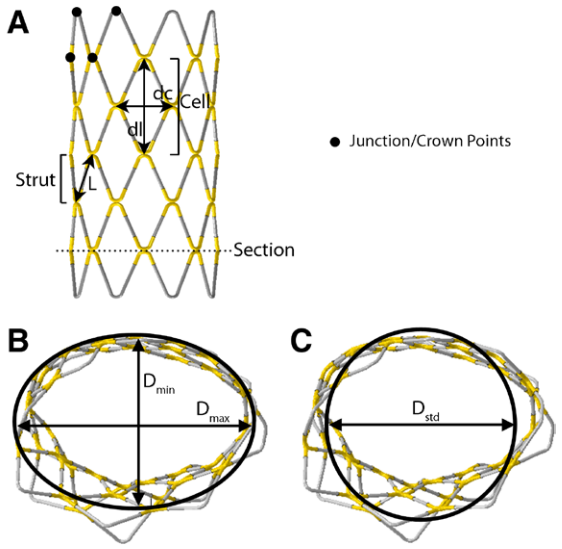

Figure 2. Stent levels and parameters identified for the 3-dimensional geometric analysis: strut length (L), cell longitudinal (dl), and circumferential (dc) diagonals, maximum (D_{max}), minimum (D_{min}), and standard diameter (D_{std}).

FE Modeling

The stent geometries reconstructed from the fluoroscopy images were used to implement a patient-specific PPVI FE model for each case. The reconstructed stents from the 3 instants (prerecoil, systole, and diastole) were superimposed to the stent geometry in its initial configuration, while still crimped onto the balloon catheter (Figure 1B) using a partial procrustes analysis. This allowed us to measure the displacements of every junction point from its initial position to the prerecoil state, and to systole and diastole reducing stent rigid displacements because of heart beating and respiration motions. Such displacements were used as boundary conditions to deploy the FE model of the PPVI stent computationally. In this study, the presence of the biological valve housed inside the stent frame was not taken into account.

A structured hexahedral mesh (792 640 solid elements with reduced integration: 658 560 for the platinum/10% iridium core and 134 080 for the golden reinforcements) was chosen after sensitivity analysis (Figure 3). Previously reported material properties

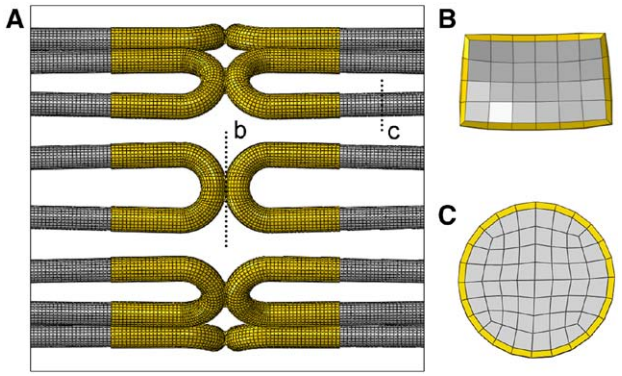

Figure 3. Finite element model of the Melody device: details of the structured hexahedral mesh (**A**), and mesh features at the welding links (**B**) and at the wire section (**C**).

Table 2. Number of Fractured Struts for Each Patient at 1-, 6-, 9-, and 12-Month Follow-Up X-Ray Examination; Fracture Type at Year 1; Maximum Doppler Gradients Immediately After PPVI and at 1-Year Follow-Up

Patient	1 mo	6 mo	9 mo	1 y	Fracture Type at 1 y[2]	Fracture Progression	Gradient Immediately After PPVI	Gradient at 1 y Follow-Up
1	0	3	NA	8	II	NA	25	NA*
2	0	2	2	2	I	NA	10	21
3	NA	NA	NA	5	II	NA	36	22
4	0	0	0	1	I	NA	19	37
5	0	1	1	1	I	NA	36	25
6	NA	NA	NA	2	I	2 (2 y)	46	57
7	NA	NA	4	NA	I	11 (2 y)	41	43 (2 y)
8	NA	NA	NA	1	I	4 (3 y)	29	29
9	1	1	1	1	I	NA	31	57
10	0	0	NA	1	I	3 (3 y)	22	29

NA indicates not available; and PPVI, percutaneous pulmonary valve implantation.
*Difficult imaging window: homograft and pulmonary artery not well seen.

were used for the platinum/10% iridium alloy stent and for the gold reinforcements.[9]

The commercial software Abaqus/Standard (Simulia, Providence, RI) was used to run the simulations. A symmetrical initial stress condition formerly calculated was assigned to the stent model to account for residual stresses caused by the loading of the stent onto the catheter balloon in the catheterization laboratory. The displacements calculated from the fluoroscopy reconstruction superimpositions were applied to the central node of the wire sections, for the outer crowns, and of the welding links, for the internal crowns (Figure 3B and 3C). The simulations included 3 steps for each patient. First, the stent was expanded from its initial crimped status to the final configuration at the end of balloon inflation. Then, displacements recorded during systole and diastole were replicated.

Stress Parameters

The following 4 parameters were analyzed for each stent at 10 equally spaced increments during recoil (end of balloon inflation to end of balloon deflation) and during cardiac cycle (systole to diastole):

- Maximum principal stress (positive): maximum and average values.
- Minimum principal stress (negative): minimum and average values.

Statistical Analysis

Univariate binary logistic regression was used to estimate the odds ratio of stent fracture, using the binary fractured/nonfractured outcomes as response variables. The explanatory variables considered in this analysis included the geometric parameters at systole, during recoil and during the cardiac cycle (21 variables), and the stress parameters measured in the FE simulations during recoil and the cardiac cycle (8 variables).

To assess the independence of the relationships in the case of multiple significant associations, a stepwise, forward conditional multivariable binary logistic regression analysis was used with consideration of variables with a P value <0.05 on univariate analysis. The likelihood ratio test was performed to gauge the contribution of individual parameters to the resulting models, and the Nagelkerke R^2 was calculated to assess the appropriateness of the model fit. In this way, the covariates that were associated with higher or lower risk of fracture were identified. The analysis was performed in the commercial software IBM SPSS Statistics (IBM Corp, New York, NY).

Results

Reconstruction From Fluoroscopy Data and Geometric Parameters

Patient data are summarized in Table 1, including some clinical and radiographic parameters previously reported to be associated to the risk of stent fracture. The in situ 3D stent geometry from fluoroscopy images was reconstructed for all 42 patients at the 3 time points. Full elaboration of each set of biplane images took ≈4 hours. Fractures were not detected immediately after the procedure. Subsequent fractures are summarized in Table 2. For every patient, ≥1 strut was selected for calibration purposes, and for those patients where a post-dilatation balloon was used, the maximum difference between the 2 calibration methods (strut based and marker based) was 4.6%. The maximum reconstruction process error was 5.9% (Figure 4). The geometric parameter results are reported in Table 3.

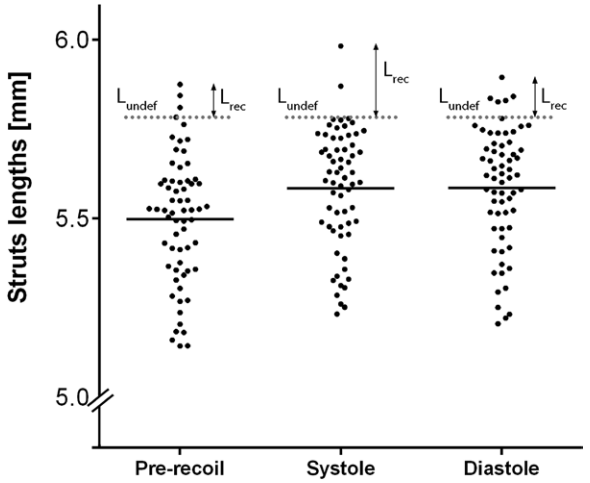

Figure 4. Distribution around the mean (continuous line) of the strut lengths reconstructed for 1 patient at prerecoil, systole, and diastole (enlarged y-axis scale). The undeformed strut length (L_{undef}=5.78 mm) is represented by the dotted lines. L_{rec} indicates the largest reconstruction error.

Table 3. Geometric Parameter Results (Average [Min, Max])

	Fractured			Nonfractured		
	Prerecoil	Systole	Diastole	Prerecoil	Systole	Diastole
L, mm	5.52 [4.89, 6.10]	5.52 [4.91, 6.06]	5.51 [4.98, 6.03]	5.48 [4.42, 6.06]	5.50 [4.36, 6.12]	5.49 [4.39, 6.12]
C_a	1.16 [0.46, 3.31]	1.26 [0.55, 4.24]	1.26 [0.55, 3.85]	1.21 [0.35, 3.83]	1.29 [0.37, 4.12]	1.29 [0.37, 3.99]
R_a	1.09 [1.02, 1.32]	1.20 [1.01, 1.88]	1.20 [1.01, 1.89]	1.09 [1.01, 1.26]	1.13 [1.01, 1.54]	1.13 [1.01, 1.60]
L_a	1.19 [1.06, 1.38]	1.21 [1.07, 1.38]	1.21 [1.06, 1.39]	1.21 [1.05, 1.35]	1.24 [1.04, 1.42]	1.23 [1.04, 1.42]

FE Analysis

In some cases, the displacement condition applied to the nodes to expand the stent resulted in distortion of the elements surrounding these nodes. To overcome this problem, the set of elements around the displacement nodes was subtracted from the model in the postprocessing of the stress results. Because the PPVI stent was modified to add gold brazing to the welds, fractures at the welding junctions have not been reported for the PPVI stent; therefore, this subtraction was considered acceptable.

The stress parameter results are reported in Table 4. The maximum values of the equivalent Von Mises and maximum principal stresses were located for every patient in different struts, but always close to the strut junctions, where bending concentrated (Figure 5), and always during the cardiac cycle. The minimum value of the minimum principal stress (negative stress) occurred close to the strut junctions, usually where the maximum Von Mises stress was registered. The minimum Von Mises stresses were usually seen in the straight segments (Figure 5).

Statistical Analysis

Univariate logistic regression of the 7 families of geometric parameters identified the maximum change in the radial asymmetry ΔR_a after balloon deflation (Figure 6) as associated with the risk of fracture (Table 5). This means that a preserved stent circularity after deployment was associated with a decreased probability of fracture (odds ratio, 0.98; 95% confidence interval, 0.96–0.99; *P*=0.006). Fracture occurred in the section with maximum change in circularity after recoil in 7 of 10 patients, whereas in the other 3 patients, it happened 2 to 4 sections next to the fractured one.

Univariate analysis of the FE data identified the minimum values of the minimum principal stresses (negative stress) during recoil (odds ratio, 0.98; 0.96–0.997; *P*=0.03) as associated with the risk of fracture (Table 6). This means that large compressive stresses during balloon deflation are associated with a higher risk of fracture.

A multivariable logistic regression model was used to assess if the 2 associations identified on univariate analysis were independent. In this model, the 2 covariates (1 geometric and 1 FE) were found to be independently associated with the risk of fracture (Tables 7 and 8). The resultant statistical model correctly identified fracture or no fracture in 93% of patients, with sensitivity 0.90 (95% confidence interval; 0.55–0.98) and specificity 0.94 (95% confidence interval, 0.79–0.99; Tables 7 and 8).

Discussion

Fracture is a well-known complication of the PPVI Melody stent occurring in ≤25% of patients.[2,3,5] This is reflected also by our series of patients (n=42), where 24% of the cases (n=10) experienced fracture in the first year after implantation. However, the reasons for fracture have not been fully identified, and the occurrence of this adverse event is likely because of a complex interaction between patient and device factors.

In this study, we categorized and evaluated 3D fundamental geometric and engineering parameters that could relate to stent fracture. The set of parameters selected takes into account, among others, all the clinical risk factors previously identified by Nordmeyer et al[2] and McElhinney et al[3]: morphological characteristics of the RVOT, presence of a BMS or calcification in the conduit, location of the device in respect to the sternum, stent recoil after balloon deflation, post-PPVI dilatation with a high pressure balloon, and asymmetries in the expanded device. All these influence the stent final geometry and behavior during balloon deflation and cardiac cycle. The geometry and variation in geometry were fully characterized by dividing the stent in sublevels, whereas the mechanical effects of each stent final shape and deformation were reflected in the stress distribution.

Logistic regression analysis was used to identify covariates affecting the odds of stent fracture. In this study, we identified both geometric and FE variables that were associated with the risk of fracture. Multivariable logistic regression confirmed the independent association of geometric and FE variables, and the resultant statistical model correctly identifying fracture or no fracture in 93% of patients.

The change in the stent section shape after balloon deflation was the most influential variable affecting the odds of stent fracture: the balloon deployment forces, the implantation site, and therefore, the stent toward a cylindrical geometry, which

Table 4. Stress Parameter Results (Average [Min, Max])

	Fractured		Nonfractured	
MPa	Recoil	Cardiac Cycle	Recoil	Cardiac Cycle
Max prin stress, max	607.49 [572.06, 655.23]	661.69 [620.77, 743.70]	599.03 [548.29, 658.22]	636.00 [565.75, 769.37]
Max prin stress, aver	113.38 [105.31, 119.05]	85.15 [76.20, 98.71]	114.93 [110.00, 119.39]	85.13 [74.28, 110.51]
Min prin stress, min	−594.88 [−667.39, −495.54]	−664.78 [−723.45, −615.60]	−553.49 [−625.05, −475.40]	−663.71 [−878.97, −571.78]
Min prin stress, aver	−90.89 [−94.85, −83.87]	−86.23 [−98.73, −75.35]	−92.19 [−102.83, −88.66]	−85.33 [−111.54, −76.52]

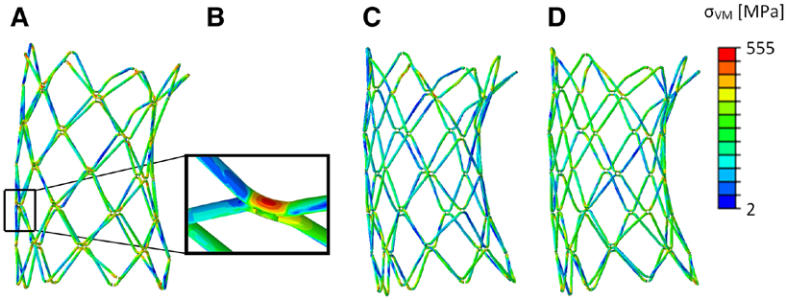

Figure 5. Von Mises stress (σ_{VM}) distribution at the end of the balloon expansion (**A**), systole (**C**), and diastole (**D**). Zoom in correspondence of the strut intersection opening to show the elements with highest stress (**B**).

may change after balloon deflation because of the recoil of the conduit and external influences. This can cause the stent sections to deform to an elliptical shape. We found that the lesser the shape of a given section of the stent changes the lower the risk of frame fracture. In general, 3D static asymmetries of the stent frame and variation during the cardiac cycle seemed not to be strongly correlated with fracture, whereas dynamic changes in the stent, and presumably the implantation site, after deployment were associated with higher risk of stent fracture. This is indeed supported by a recent study reporting on balloon-expandable stent implantation in systemic outflow tracts, which resulted in fractures in 43% of the cases.[14] These results are consistent with the clinical findings that prestenting is associated with a lower probability of fracture[15]: in the study of Nordemeyer, the incidence of fractures in prestented patients was 21%, whereas other groups reported lower rates[3,8,16] or no frequency. The differences between these studies may be because of the type of prestent used, the number of prestent implanted, and whether the BMS was already present before the PPVI procedure or was placed during the same catheterization. In our cohort of patients, all prestents (MaxLD, EV3, Plymouth, MN) were implanted during the same catheterization as the PPVI; the median number of prestents per patient was 1, with only 3 patients having 2 BMS placed with an overlap portion along their length. The prestents did not present evident fractures before Melody deployment and full apposition of the Melody stent within the BMS was achieved in all cases. In addition, the outcomes of the present work agree with the finding in previous studies that associated heavy calcification of the conduit and no stent recoil (qualitatively assessed) with a lower probability of fracture.[2,3]

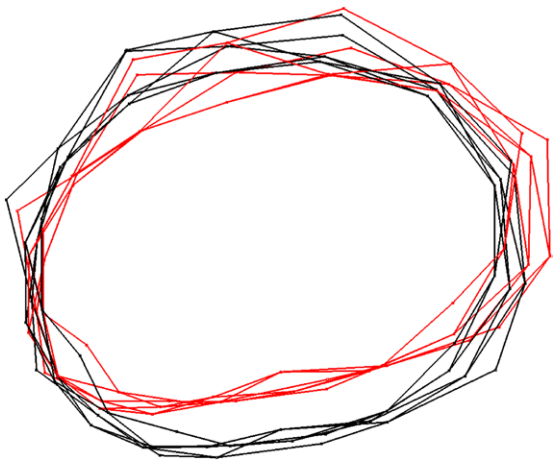

Figure 6. Change in the radial asymmetry ΔR_a from the prerecoil (black) to the systole (red) shown for 1 patient in the fluoroscopy reconstruction.

Importantly, our preliminary analysis shows that changes in PPVI shape at the time of implantation may be one of the key factors to consider when further developing predictive models for stent fracture identification. This would enable us to define specific follow-up protocols for patients. Using our set statistical criterion, we would categorize 11 patients as high risk for stent fracture with 9 patients fracturing and 2 not; hence, we would have potentially submitted 2 patients to have stringent follow-up. For the 31 patients, we would have placed in the low-risk group, 1 patient did have a fracture, but 30 patients would potentially have avoided needless follow-up.

An early, systematic biomedical analysis after device implantation has the potential to risk stratify patients accurately, defining follow-up strategies and possibly reducing expensive follow-up investigations and clinic time. Starting from these outcomes, further work is now required to implement an accurate predictive statistical tool, and to define what

Table 5. Univariate Analysis Geometric Parameters

Predictor	Odds Ratio (95% CI for OR)	*P* Value
L min systole	860 (0.1–8.6e^6)	0.2
L aver systole	1e^4 (0.02–6.9e^{10})	0.2
ΔL max recoil	1.1 (0.8–1.4)	0.5
ΔL aver recoil	1.2 (0.7–2.2)	0.5
ΔL max cardiac cycle	2e^5 (0.03–1.7e^{12})	0.1
ΔL aver cardiac cycle	0.8 (0.2–3.5)	0.8
C_a min systole	1.2 (0.01–100)	0.9
C_a aver systole	0.4 (0.1–15)	0.6
ΔC_a max recoil	0.96 (0.88–1.04)	0.3
ΔC_a aver recoil	0.9 (0.8–1.1)	0.4
ΔC_a max cardiac cycle	1.1 (0.9–1.4)	0.4
ΔC_a aver cardiac cycle	1.5 (0.4–5.9)	0.6
R_a max systole	88 (0.7–10 405)	0.07
R_a aver systole	280 (0.4–1.9e^5)	0.09
ΔRa max recoil	0.97 (0.95–0.99)	0.006
ΔR_a aver recoil	0.99 (0.98–1.0)	0.07
ΔR_a max cardiac cycle	0.99 (0.93–1.04)	0.6
ΔR_a aver cardiac cycle	1.0 (1.00–1.02)	0.06
L_a systole	0.05 (0–61)	0.4
ΔL_a recoil	1.04 (0.9–1.3)	0.7
ΔL_a cardiac cycle	0.87 (0.3–2.7)	0.8

CI indicates confidence interval; and OR, odds ratio.

Table 6. Univariate Analysis Finite Element Parameters

Predictor	Odds Ratio (95% CI for OR)	*P* Value
Max prin stress, max recoil	1.0 (0.99–1.0)	0.4
Max prin stress, aver recoil	0.84 (0.67–1.07)	0.2
Max prin stress, max cardiac cycle	1.0 (0.99–1.02)	0.2
Max prin stress, aver cardiac cycle	1.0 (0.89–1.12)	1.0
Min prin stress, min recoil	0.98 (0.96–0.997)	0.03
Min prin stress, aver recoil	1.2 (0.89–1.65)	0.2
Min prin stress, min cardiac cycle	1.0 (0.99–1.01)	1.0
Min prin stress, aver cardiac cycle	0.98 (0.88–1.09)	0.7

CI indicates confidence interval; and OR, odds ratio.

safe follow-up strategies should be used for high- and low-risk patients. To this end, the model should be extended to predict not only which patients are at high risk for fracture but also which of these fractures may become clinically significant because of loss of stent integrity. A refined FE model that includes the loading effects of implantation site and surrounding tissue could help analyze the progression of fractures for each individual case.

Limitations

Several important limitations in this study should be considered. Follow-up patient data at 1 year were available in the form of chest radiographs but no dynamic fluoroscopy images. Despite the excellent radio-opacity of the platinum iridium alloy, chest radiographs are not always optimal to visualize clearly the presence of a stent fracture, whose number may have been underestimated in this study.

The FE analysis although comprehensive did not include residual stresses caused by the asymmetrical manual crimping of the device onto the delivery catheter and by potential multiple inflations of the post-PPVI dilatation balloon. These residual stresses play an important role in fatigue phenomena but could not be estimated for our patient population.

The magnitude of stent recoil depends not only on the specific implantation site and surrounding tissue environment but also on the percutaneous technique used to deliver the stent, such as the chosen balloon size and inflation pressure. It is not possible to distinguish the effects of these 2 factors on the risk of fracture, but the influence of the overall recoil on risk for fracture is assessed with the proposed analysis.

The proposed models were developed in a relatively small cohort of 40 patients; therefore, they require validation in a prospective cohort, to overcome the inherent possibility of overfitting in a training data set. It is likely that the sensitivities and specificities are, therefore, optimistically biased. However, with these preliminary data, we have aimed for the identification of those variables that might need further analysis and that could be at the basis of a predictive model with statistical significance. In the present work, we tried to reduce the risk of overfitting limiting the explanatory covariates (1 from the geometric model and 1 from the FE model) and generating simple and parsimonious models, with limited explanatory covariates.

Finally, the 3D reconstruction process and measurement of the parameters predictors for fracture currently require technical image processing, unavailable in many clinical environments. Translation of this process to the clinical environment will be aided by automated image processing techniques, to create user-friendly tools easily accessible to clinicians.

Clinically, all Melody stent fractures are not necessarily significant, and in these analyses, we did not differentiate between major and minor fractures. This study was not designed to assess factors associated with hemodynamically significant stent fractures, but will hopefully provide a foundation for further investigations toward that end.

Table 7. Multivariable Logistic Regression Analysis of 42 Patients at 1-Year After PPVI: Geometric and Finite Element Parameters

	Geometric and Finite Element Parameters*					
Explanatory Variables	β	SE β	Wald χ^2	df	*P* Value	OR (95% CI for OR)
Constant	−51.75	21.2	5.96	1	0.015	NA
ΔR_a max at recoil	−0.076	0.03	6.71	1	0.010	0.927 (0.875–0.982)
Min values of min princ stresses during recoil	−0.078	0.03	5.71	1	0.017	0.924 (0.866–0.986)
Test			χ^2	df	*P* Value	
Overall model evaluation						
Omnibus tests of coefficients			29.4	2	<0.00001	
Goodness-of-fit test						
Hosmer and Lemeshow			3.45	8	0.903	

CI indicates confidence interval; NA indicates not available; OR, odds ratio; and PPVI, percutaneous pulmonary valve implantation.

*−2 log likelihood=16.68; Nagelkerke R^2=0.756, Cox and Snell R^2=0.504.

Conclusions

Stent fracture is a common adverse event after Melody PPVI and other stent implantation. For this reason, patients require careful follow-up to ensure that device/stent integrity remains. This study highlights that asymmetries in stent section geometry and cells shape, particularly during recoil after balloon deflation, are important variables associated with stent fracture. We have proposed a parsimonious statistical model based on 3D geometric and stress analysis, to identify whether a

Table 8. Observed and Predicted Frequencies of Fracture for PPVI Using the Geometric and Finite Element Parameters by Logistic Regression With Cutoff of 0.30

	Predicted Fracture*		
Observed Fracture	No	Yes	% Correct
No	30	2	93.8
Yes	1	9	90.0
Overall	…	…	92.9

CI indicates confidence interval; and PPVI, percutaneous pulmonary valve implantation.

*Sensitivity=0.90 (confidence interval, 0.55–0.98), specificity=0.94 (confidence interval, 0.79–0.99), false-positive=18.2%, false-negative 3.2%.

PPVI patient is likely to incur a subsequent stent fracture. Such model will require prospective validation but could be used to risk stratify patients and to plan bespoke clinical follow-up strategically.

Acknowledgments

This report is independent research from the National Institute for Health Research Biomedical Research Centre Funding Scheme. The views expressed in this publication are those of the author(s) and not necessarily those of the National Health Service, the National Institute for Health Research or the Department of Health.

Sources of Funding

This research is funded by the European Commission through the MeDDiCA ITN (http://www.meddica.eu; PITN-GA-2009–238113), Marie Curie actions under FP7, People Programme, the British Heart Foundation, the Royal Academy of Engineering/EPSRC, the National Institute of Health Research, the Rosetrees Trust and Heart Research United Kingdom.

Disclosures

Dr Bonhoeffer has served as a consultant to Medtronic and NuMed. Drs Taylor and Schievano have served as consultants to Medtronic. The other authors report no conflicts.

References

1. Lurz P, Bonhoeffer P, Taylor AM. Percutaneous pulmonary valve implantation: an update. *Expert Rev Cardiovasc Ther*. 2009;7:823–833.
2. Nordmeyer J, Khambadkone S, Coats L, Schievano S, Lurz P, Parenzan G, Taylor AM, Lock JE, Bonhoeffer P. Risk stratification, systematic classification, and anticipatory management strategies for stent fracture after percutaneous pulmonary valve implantation. *Circulation*. 2007;115:1392–1397.
3. McElhinney DB, Cheatham JP, Jones TK, Lock JE, Vincent JA, Zahn EM, Hellenbrand WE. Stent fracture, valve dysfunction, and right ventricular outflow tract reintervention after transcatheter pulmonary valve implantation: patient-related and procedural risk factors in the US Melody Valve Trial. *Circ Cardiovasc Interv*. 2011;4:602–614.
4. Nordmeyer J, Coats L, Lurz P, Lee TY, Derrick G, Rees P, Cullen S, Taylor AM, Khambadkone S, Bonhoeffer P. Percutaneous pulmonary valve-in-valve implantation: a successful treatment concept for early device failure. *Eur Heart J*. 2008;29:810–815.
5. Fleming GA, Hill KD, Green AS, Rhodes JF. Percutaneous pulmonary valve replacement. *Prog Pediatr Cardiol*. 2012;33:143–150.
6. McElhinney DB, Hellenbrand WE, Zahn EM, Jones TK, Cheatham JP, Lock JE, Vincent JA. Short- and medium-term outcomes after transcatheter pulmonary valve placement in the expanded multicenter US melody valve trial. *Circulation*. 2010;122:507–516.
7. Nordmeyer J, Lurz P, Khambadkone S, Schievano S, Jones A, McElhinney DB, Taylor AM, Bonhoeffer P. Pre-stenting with a bare metal stent before percutaneous pulmonary valve implantation: acute and 1-year outcomes. *Heart*. 2011;97:118–123.
8. Butera G, Milanesi O, Spadoni I, Piazza L, Donti A, Ricci C, Agnoletti G, Pangrazi A, Chessa M, Carminati M. Melody transcatheter pulmonary valve implantation. Results from the registry of the Italian Society of Pediatric Cardiology. *Catheter Cardiovasc Interv*. 2013;81:310–316.
9. Schievano S, Petrini L, Migliavacca F, Coats L, Nordmeyer J, Lurz P, Khambadkone S, Taylor AM, Dubini G, Bonhoeffer P. Finite element analysis of stent deployment: understanding stent fracture in percutaneous pulmonary valve implantation. *J Interv Cardiol*. 2007;20:546–554.
10. Schievano S, Taylor AM, Capelli C, Lurz P, Nordmeyer J, Migliavacca F, Bonhoeffer P. Patient specific finite element analysis results in more accurate prediction of stent fractures: application to percutaneous pulmonary valve implantation. *J Biomech*. 2010;43:687–693.
11. Vano E, Geiger B, Schreiner A, Back C, Beissel J. Dynamic flat panel detector versus image intensifier in cardiac imaging: dose and image quality. *Phys Med Biol*. 2005;50:5731–5742.
12. Cosentino D, Zwierzak I, Schievano S, Díaz-Zuccarini V, Fenner JW, Narracott AJ. Uncertainty assessment of imaging techniques for the 3D reconstruction of stent geometry. *Med Eng Phys*. 2014;36:1062–1068.
13. Porras D, McElhinney DB, Del Nido P, Lock JE, Meadows J, Marshall AC. Clinical and stent-related outcomes after transcatheter or operative placement of bare-metal stents in the ventricular septum or subvalvar systemic outflow tract. *Circ Cardiovasc Interv*. 2012;5:570–581.
14. Boudjemline Y, Brugada G, Van-Aerschot I, Patel M, Basquin A, Bonnet C, Legendre A, Bonnet D, Iserin L. Outcomes and safety of transcatheter pulmonary valve replacement in patients with large patched right ventricular outflow tracts. *Arch Cardiovasc Dis*. 2012;105:404–413.
15. Eicken A, Ewert P, Hager A, Peters B, Fratz S, Kuehne T, Busch R, Hess J, Berger F. Percutaneous pulmonary valve implantation: two-centre experience with more than 100 patients. *Eur Heart J*. 2011;32:1260–1265.
16. Demkow M, Biernacka EK, Spiewak M, Kowalski M, Siudalska H, Wolski P, Sondergaard L, Miśko J, Hoffman P, Rużyłło W. Percutaneous pulmonary valve implantation preceded by routine prestenting with a bare metal stent. *Catheter Cardiovasc Interv*. 2011;77:381–389.